04

Microchannel structure of a spark discharge in a „ pin to plane “ gap at different air pressures

© *A.A. Trenkin, K.I. Almazova, A.N. Belonogov, V.V. Borovkov, E.V. Gorelov, A.S. Dolotov*

Russian Federal Nuclear Center, All-Russia Research Institute of Experimental Physics,
Sarov, Russia
e-mail: alexey.trenkin@gmail.com

Received July 17, 2022
Revised August 9, 2022
Accepted August 10, 2022

Using high-speed photography and shadow photography, the structure of the glow and the microstructure of the spark discharge in a 1.5 mm long „pin(cathode)-plane“ gap in air in the pressure range from 300 to 760 Torr has been studied. The presence of a microchannel structure of the discharge in the indicated pressure range was established — the discharge is a aggregation of a large number of micron-diameter channels. It is shown that with decreasing pressure, the evolution of the microstructure and glow of the discharge lags behind the onset of breakdown, however, their morphology retains similarity at different pressures

Keywords: spark discharge, microstructure, method of shadow photography, high-speed shooting.

DOI: 10.21883/TP.2022.11.55173.184-22

Introduction

Studies of discharges in air have been conducted for a long time, but are still very relevant today. In addition to a purely scientific interest, this is due to a number of other reasons. First, air is the natural atmosphere in which various electrical phenomena of inartificial (e.g., lightning) and technogenic (e.g., short circuits) origin occur. Second, air at various pressures is the operating medium in some gas-discharge technologies of practical importance.

In studies of different types of discharges in atmospheric pressure air, a microstructure was found, where the channel is an aggregate of a large number of microchannels (filaments) [1–6]. It was found that the microstructure arises in the initial phase of the discharge, and its formation apparently occurs due to the instability of the ionization wave front [1,7–13]. It was also shown that the presence of the microstructure can provide a number of specific effects that are absent in structureless (uniform) channels: generation of high-energy electrons in microchannels, acceleration of microstructured channel heads, elevated electron temperatures, etc. [4,14,15].

In this connection, it is of scientific and practical interest to expand the conditions for realization of gas discharges in order to determine the microstructure presence in them. This paper presents the results of spark discharge studies in the pressure range from 300 to 760 Torr. Note, that this range corresponds to the interval of heights from the ground surface to about 7 km, in which lightning discharges [16] are realized.

1. Experimental equipment and procedures

The diagram of the experimental bench is presented in Fig. 1. A part of its elements are characterized in detail in [3,4]. Pulsed voltage generator ensured negative polarity output pulse with an amplitude of 25 kV and a 0.1–0.9 rise time of approximately 7 ns. The pulse was applied to discharge gap through the cable line. Voltage and current measurements were performed at the pulsed voltage generator output by means of a capacitance divider and resistive shunt, accordingly. The temporalfresolution of the divider and the shunt was —no worse than 1 ns. Signals were recorded using an oscilloscope with a bandwidth of 500 MHz and a digitizing rate of 2 GS/s.

The electrode system had a „pin–plane“ geometry. An axially symmetric pin electrode is fabricated from stainless steel and had a length of 50 mm, diameter of 14 mm, an

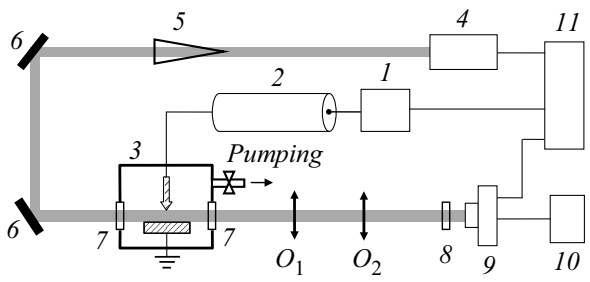

Figure 1. Diagram of the experimental stand: *1* — voltage pulse generator, *2* — cable line, *3* — vacuum chamber with an electrode system, *4* — sounding signal source (laser), *5* — collimator, *6* — turning mirror, *7* — window, O_1 and O_2 — lenses, *8* — light filters, *9* — electron-optical recorder, *10* — personal computer, *11* — synchronization unit.

apex angle of 36°, and a curvature radius of 0.15 mm. A plane electrode was fabricated from an aluminum alloy and had the working part close in shape to a segment of a sphere with a diameter of 4.5 cm and a thickness of 1.5 cm. The interelectrode gap was 1.5 mm.

The electrode system was placed coaxially inside a cylindrical metal vacuum chamber. Chamber diameter is 310 mm, height is 800 mm. Input and output of laser radiation was carried out through chamber windows made of KU-1 glass with a diameter of 80 mm and a thickness of 15 mm. The vacuuming system provided an operating gas pressure in the chamber from atmospheric to Torr units.

An optical detection system was used as a part of the bench. The system included a probing radiation source — solid-state laser (wavelength of 532 nm and a half-height pulse duration at 6 ns), collimator, lenses, light filters, and digital electron-optical camera. A plane-parallel laser beam crossed the discharge region at a right angle to the spike–electrode axis and was detected by the electron-optical camera. The laser beam at the discharge generation region had a crosswise size of approximately 1 cm and a Gaussian profile. Due to the presence of a vacuum chamber in the present experiments, the optical scheme was changed by adding a second lens, in contrast to the earlier experiments [3,4]. The O_1 lens, located at double focal distance from the discharge gap, made its image in scale of 1 : 1. Then lens O_2 transferred this image with magnification (scale 10 : 1) to the photocathode of the electron-optical recorder.

Shadow shooting methodology is based on this system. The exposure of each frame was set by the laser pulse duration. The frameswere timed relative to the moment of breakdown, and the time characterizing them corresponds to the start of imaging.

The laser was not used in the experiments on shooting the intrinsic glow of the discharge. The frame exposure of the electron-optical recorder was 40 ns. When shooting the early stages of the discharge (at times below 40 ns), part of the exposure time was ahead of the beginning of the discharge formation. The linking of the frame of the intrinsic glow discharge was determined by the moment of the shutter closing of the electron-optical camera.

The registration system worked in single-frame mode — i. e. one frame per pulse. Different stages of the discharge process were visualized by shifting the moments of actuation of the laser and the electron-optical detector relative to the moment of breakdown. The resolving power of the optical system was 5 μm per three pixels.

2. Experimental results and discussion

Based on the results of earlier studies [3] of a discharge in air at atmospheric pressure, we note its main characteristics. An oscillatory process with exponential current and voltage decay was initiated in the discharge circuit after the breakdown of the gap. The oscillation period was 0.6 μs, and

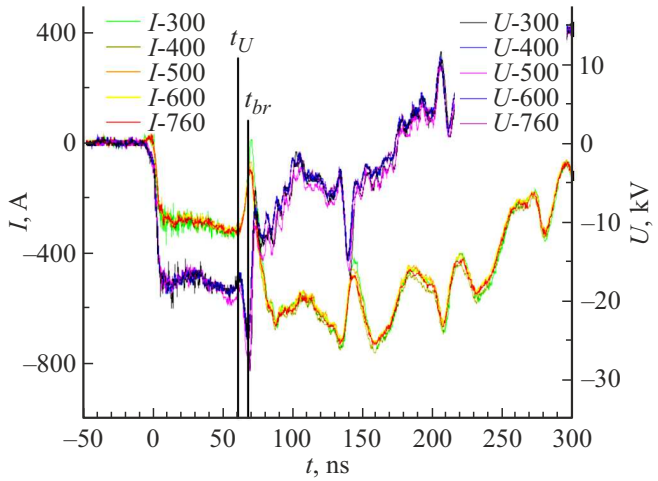

Figure 2. Initial fragments of voltage U and current I oscillograms at different pressures (t_U — moment of voltage appearance across the discharge gap; t_{br} — moment of breakdown).

the amplitude and the decay time of current were — 1 kA and 1.2 μs, respectively. At the same time, two characteristic moments were distinguished on oscillograms: occurrence of voltage within the discharge gap t_U and breakdown. The onset of the current rise (and the voltage decay) was assumed to be the moment of breakdown t_{br}.

In experiments [3], the following dynamics of the spatial structure of the initial phase of the discharge was registered. In the pre-breakdown stage a weakly luminous diffuse channel and cathode spots appear, then in the interval from 5 to 15 ns, luminous formations propagate from the cathode, and the gap is closed by a uniform, brightly luminous channel. The shadow patterns show that the channel is a cluster of a large number of microchannels, which are unresolvable in the discharge glow photographs. The microstructure is registered on the shadow patterns from the first nanoseconds after the breakdown.

Fig. 2 shows the initial fragments of voltage U and current I oscillograms at various pressures. In the time interval from 0 to 60 ns, electrical signals propagate along the cable line. The rise of voltage and current decreasing in the interval between t_U and t_{br} corresponds to the voltage wave reflection from the initially open end of the cable line. It can be seen that the discharge voltage and current realized at the indicated pressures have no significant differences.

Fig. 3 shows photographs of the discharge glow at 300 Torr pressure at different moments of time. Let us compare the dynamics of the luminescence registered here at a pressure of 300 Torr and at a pressure of 760 Torr, studied in detail in [3].

Morphologically, the discharge develops in the same way, but there is a delayed phase of development with a decrease in pressure. Thus, cathode spots without spark channel development at 300 Torr exist up to 10 ns, while the phase of their existence at 760 Torr is the pre-breakdown stage (it corresponds to the minus sign in the frame time

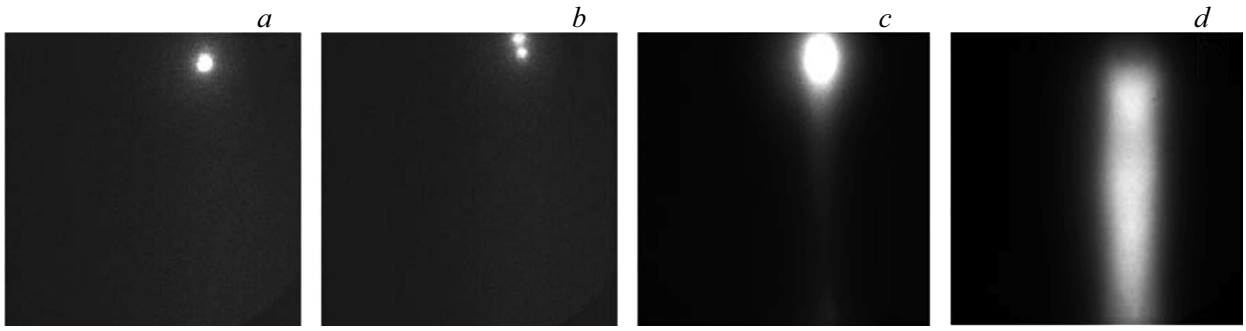

Figure 3. Photographs of the discharge glow at 300 Torr at the time: *a* — −1, *b* — 10, *c* — 20, *d* — 60 ns.

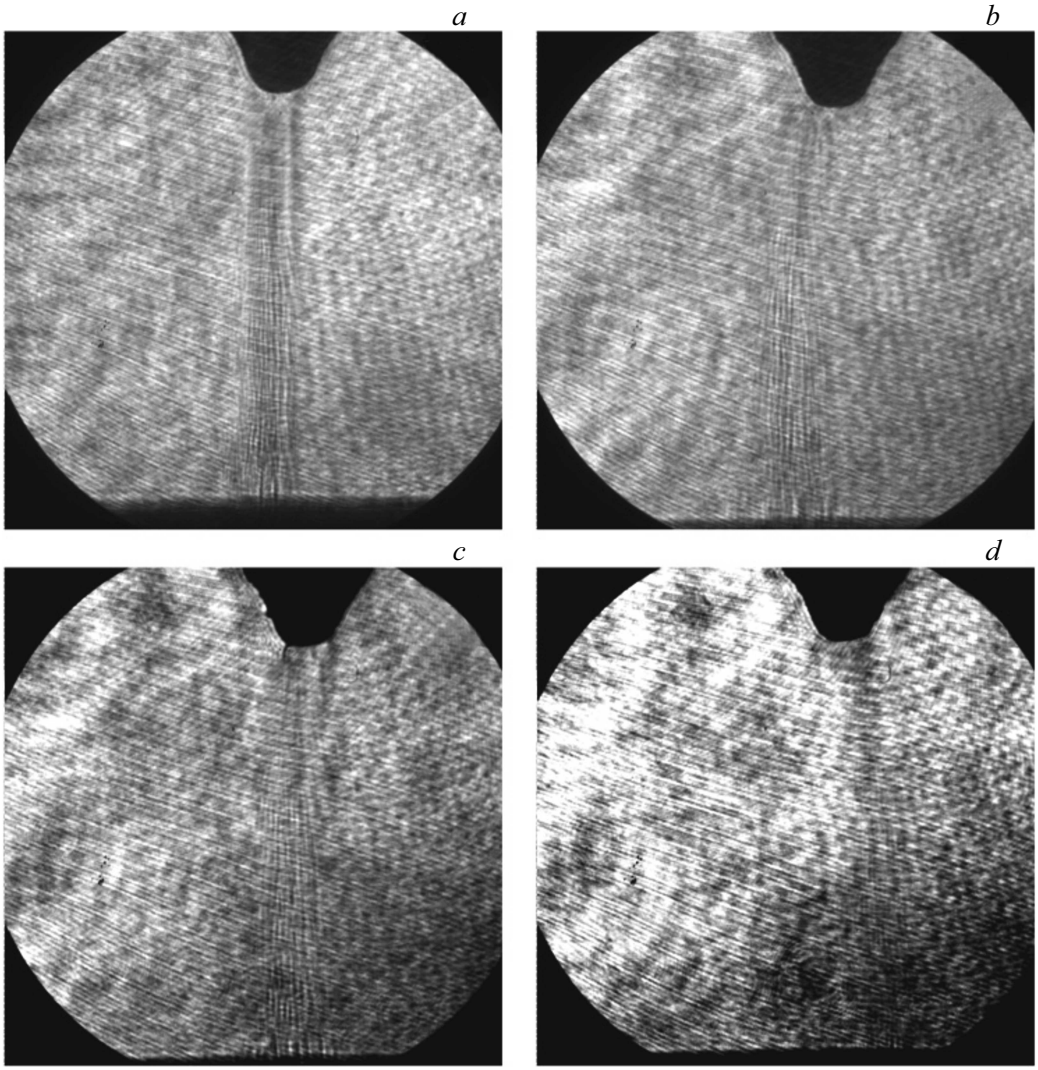

Figure 4. Discharge shadow patterns at a time of about 10 ns after breakdown at different pressures: *a* — 760, *b* — 600, *c* — 500, *d* — 400 Torr.

notation) and 1−3 ns after breakdown. A bright luminous homogeneous channel at 300 Torr is formed by 60 ns, whereas at atmospheric pressure it is formed by 15 ns. Also, less clear at lower pressures is the channel boundary at its radial expansion, which at atmospheric pressure has a higher contrast, determining the structure of the cylindrical shock wave.

Fig. 4 shows the discharge shadow patterns at different pressures in the range from 760 to 400 Torr, corresponding to approximately the same moment of time after break-

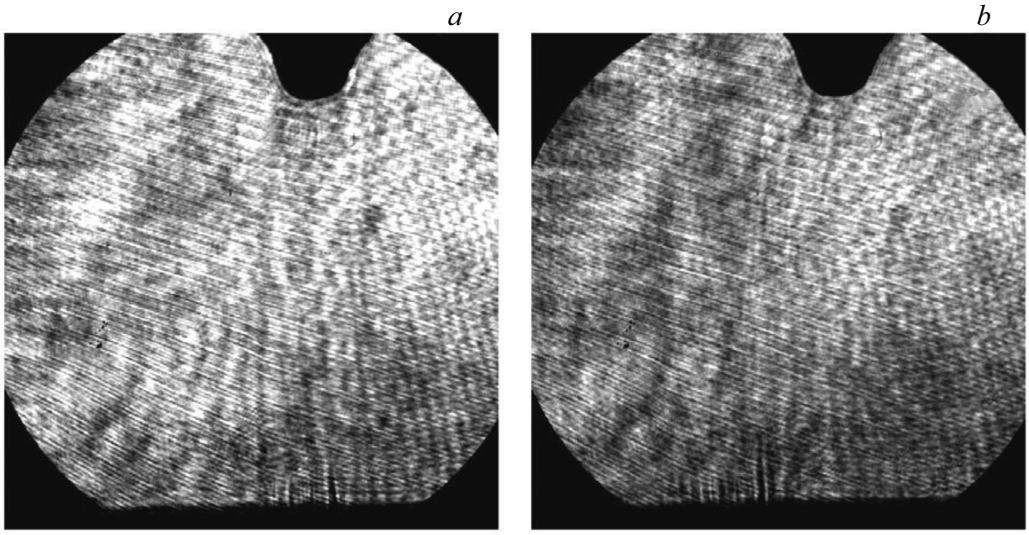

Figure 5. Discharge shadow patterns at 300 Torr at time 30 (a) and 40 ns (b) after breakdown.

down — 10 ns. All shadow patterns show a microchannel structure. The diameters of the microchannels in the central part of the discharge gap range from 10 to 15 μm, and their presence is observed from the first nanoseconds after breakdown. At the same time, some delay with respect to the breakdown phase of the discharge microstructure development with pressure decrease is noticeable. Thus, at a pressure of 400 Torr the microstructure only begins to appear and is weakly distinguishable compared to higher pressures. This circumstance becomes especially significant at pressures of 300 Torr.

Figure 5 shows the discharge shadow patterns at a pressure of 300 Torr at different moments of time after the breakdown. At this pressure, microchannels are not observed in the early stages of the shadow pattern and begin to be registered starting from 30 ns, after the breakdown. At lower pressures, the discharge structure could not be registered by the shadow shooting technique used here, which may be due to an unacceptable decrease in the gas density and its gradients beyond the sensitivity limit of the technique.

Thus, taking into account the aspects noted in the introduction, we can draw the following conclusions about the results obtained.

The main one is the presence of spark discharge microstructure not only at atmospheric, but also at lower pressures. This fact illustrates the universality of the phenomenon of discharge microstructuring, which, apparently, is associated with the basic laws of the course of gas-discharge processes. In this connection, based on the presence of microstructure in relatively long (up to 60 cm) spark channels of laboratory discharges [17], the results of the present work indicate the possibility of microstructure in more large-scale phenomena of atmospheric electricity, such as lightning, because the range of pressures studied here corresponds to the interval of heights where they are realized. Note, that the possibility of microstructuring of the lightning channel was pointed out earlier in works [17–19].

In addition, the results of this work make it necessary to take into account the presence of microstructure and related effects in the design and application of gas-discharge technologies, which use spark discharges at reduced pressures.

Conclusion

The luminescence structure and microstructure of the spark discharge in the spike (cathode)–plane length of 1.5 mm in air in the pressure range from 300 to 760 Torr was investigated using speed imaging and shadow shooting method.

The presence of a microchannel discharge structure in the investigated pressure range from the first nanoseconds after breakdown is shown: the discharge is a set of a large number of microchannels with diameters from 10 to 15 μm.

It was established that the phases of microstructure development and discharge luminescence are delayed relative to the onset of breakdown with decreasing pressure. At the same time, the morphology of these structures in the dynamics of the discharge process retains similarity at different pressures.

Conclusions are made about the possibility of microstructuring of the lightning discharge and the need to take into account the presence of microstructure in applied gas-discharge technologies using spark discharges at reduced pressures.

Conflict of interest

The authors declare that they have no conflict of interest.

References

[1] V.I. Karelin, A.A. Trenkin. Tech. Phys., **53** (3), 314 (2008). DOI: 10.1134/S1063784208030055
[2] A.G. Rep'ev, P.B. Repin, V.S. Pokrovski'. Tech. Phys., **52** (1), 52 (2007).
[3] A.A. Trenkin, K.I. Almazova, A.N. Belonogov, V.V. Borovkov, E.V. Gorelov, I.V. Morozov, S.Yu. Kharitonov. Tech. Phys., **65** (12), 1948 (2020). DOI: 10.1134/S1063784220120270
[4] K.I. Almazova, A.N. Belonogov, V.V. Borovkov, V.S. Kurbanismailov, Z.R. Khalikova, P.Kh. Omarova, G.B. Ragimkhanov, D.V. Tereshonok, A.A. Trenkin. Phys. Plasmas, **27**, 123507 (2020). DOI: 10.1063/5.0026192
[5] E.V. Parkevich, M.A. Medvedev, A.I. Khirianova, G.V. Ivanenkov, A.S. Selyukov, A.V. Agafonov, K.V. Shpakov, A.V. Oginov. Plasma Sources Sci. Technol., **28**, 125007 (2019). DOI: 10.1088/1361-6595/ab518e
[6] E.V. Parkevich, M.A. Medvedev, G.V. Ivanenkov, A.I. Khirianova, A.S. Selyukov, A.V. Agafonov, Ph.A. Korneev, S.Y. Gus'kov, A.R. Mingaleev. Plasma Sources Sci. Technol., **28**, 095003 (2019). DOI: 10.1088/1361-6595/ab3768
[7] E.D. Lozanskiy, O.B. Firsov. *Teoriya iskry* (Atomizdat, M., 1975)
[8] O.A. Sinkevich. TVT, **41** (5), 695 (2003).
[9] M. Arrayas, M. Fontelos, J. Trueba. Phys. Rev. Lett., **95** (5), 165001 (2005). DOI: 10.1103/PhysRevLett.95.165001
[10] A. Rocco, U. Ebert, W. Hundsdorfer. Phys. Rev. E, **6**, 035102(R)(2002). DOI: 10.1103/PhysRevE.66.035102
[11] U. Ebert, W. Saarloos, C. Caroli. Phys. Rev. Lett., **77** (20), 4178 (1996).
[12] M. Arrayas, U. Ebert, W. Hundsdorfer. Phys. Rev. Lett., **88** (17), 174502(R) (2002). DOI: 10.1103/PhysRevLett.88.174502
[13] A. Luque, F. Brau, U. Ebert. Phys. Rev. E, **78**, 016206 (2008). DOI: 10.1103/PhysRevE.78.016206
[14] V.I. Karelin, A.A. Trenkin, I.G. Fedoseev. Phys. Atomic Nuclei, **78** (12), 1440 (2015). DOI: 10.1134/S1063778815120133
[15] V.I. Karelin, A.A. Trenkin. High Voltage Engineering, **41** (2), 1 (2015).
[16] E.M. Bazelyan, Yu.P. Raizer. *Fizika molnii i molniezashchity* (Fizmatlit, M., 2001)
[17] M.A. Medvedev, E.V. Parkevich, A.V. Oginov, S.M. Zakharov, I.S. Baidin. Short Reports on Physics at the P.N. Lebedev Physical Institute of the Russian Academy of Sciences, **48** (12) 9 (2021).
[18] A.A. Tren'kin. Tech. Phys. Lett., **36** (4), 299 (2010). DOI: 10.1134/S1063785010040036
[19] A.V. Gordeev, T.V. Loseva. Tez. dokl. XXXIII International Conference on Plasma Physics and STS (Zvenigorod, February 13–17, 2006, p. 246.)